Global NEST Journal, Vol 26, No X, pp 1-7

Characterization and calibration of a photodiode based pyranometer for solar energy applications

Jayasankar.K. C.[1], Anandhakumar G.[1*] and Kalaimurugan A.[2]
[1]Department of Electrical and Electronics Engineering, Saveetha School of Engineering, Saveetha Institute of Medical and Technical Sciences, Saveetha University, Chennai, Tamil Nadu, India–602105
[2]Department of Electrical and Electronics Engineering, Agni College of Technology, Chennai, Tamil Nadu, India–600130.
Received: 17/03/2024, Accepted: 30/04/2024, Available online: 16/05/2024
*to whom all correspondence should be addressed: e-mail: anandhakumar@saveetha.com
https://doi.org/10.30955/gnj.005921

Graphical abstract

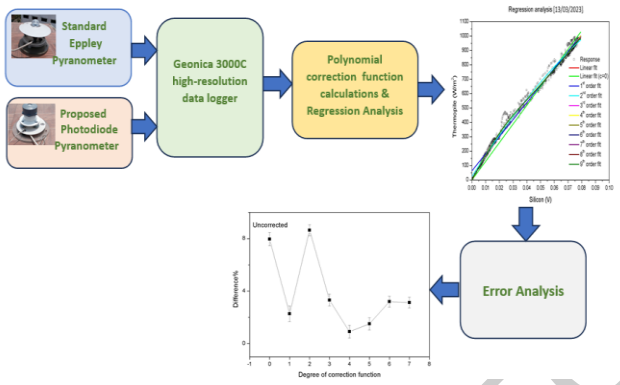

Abstract

In the realm of solar science, a pyranometer holds a pivotal role, serving as an instrument vital for the assessment of solar irradiance within the abbreviated wavelengths of the solar spectrum, spanning from 300 to 3000 nanometres. Traditional pyranometers typically employ complex and labour-intensive thermopiles. These instruments depend on sets of thermocouples linked either in series or parallel and require rare earth minerals to operate effectively. In this study, we propose a novel approach utilizing photodetectors, specifically photodiodes and phototransistors, to overcome the limitations associated with traditional pyranometers. Photodiodes, being commonly employed for this purpose, offer several advantages, including faster response times, customizable spectral range selection, and cost-effectiveness. However, they cannot entirely replace thermopiles due to challenges such as the generation of dark current in the absence of light, temperature-dependent operations, and saturation at higher irradiance levels. To address these limitations, we have developed an innovative design of a photodiode-based pyranometer that integrates a data acquisition system and correction method. This novel approach provides a viable solution for standalone solar radiation measurement, offering improved accuracy and reliability. This study compares the response of a photodiode pyranometer to a standard pyranometer on cloudy days. The photodiode pyranometer mimics the standard pyranometer's sharp declines, with transient spikes influenced by correction function magnitude. The uncorrected pyranometer overestimates irradiance, but first order linear correction mitigates this. Corrections up to seventh order result in a difference of ±10 W/m^2, suggesting third to fifth-degree corrections could be optimal. A quaternary function may be the optimal correction function, but higher order polynomials also show effectiveness.

Keywords: Dark current, data acquisition system, phototransistor, solar irradiance, thermopile

1. Introduction

Pyranometers serve as instruments to gauge solar radiation, specifically the total amount of direct and diffuse solar radiation reaching a surface. These devices play vital roles in fields such as meteorology, climatology, and solar energy research. Over time, researchers have explored ways to enhance the design and accuracy of pyranometers. In a 1998 investigation, Beaubien, Bisberg, and Beaubien delved into various aspects of pyranometer design, including material selection, sensor calibration, and the influence of environmental factors on measurement accuracy (Beaubien *et al*. 1998). Their findings offered valuable insights into pyranometer design considerations, enabling the development of more dependable instruments.

In a seminal investigation back in 2000, Bush, Valero, Simpson, and Bignone embarked upon a study delving into the thermal ramifications within pyranometers. Their endeavour delivered a corrective algorithm designed to refine the measurements of surface insolation by duly considering thermal interferences that might impinge upon pyranometer precision (Brett *et al*. 2000). An additional pivotal inquiry ensued in 2001, orchestrated by Hoefflin, Kato, Smith, Rutledge, Charlock, and Mahan. This study was laser-focused on ascertaining the thermal deviation exhibited by the Eppley Precision Spectral Pyranometer. Through meticulous quantification of this deviation, the researchers pioneered corrective

methodologies (Haeffelin *et al*. 2001). aimed at augmenting pyranometer precision.

In 2003, Wood, Muneer, and Kubie evaluated a new photodiode sensor has been developed to precisely measure both global and diffuse irradiance, alongside accurately determining sunshine duration. They aimed to assess the sensor's performance and compare it with established pyranometers (Wood *et al*. 2003). Additionally, Link, Marks, and Hardy conducted a study in 2004 on characterizing canopy radiative transfer properties using a deterministic approach. Although their research did not directly focus on pyranometers, it contributed to understanding how solar radiation interacts with vegetation and the environment (Link *et al*. 2004).

Raïch's 2007 study explored the influence of solar elevation, cloud cover, and temperature on silicon pyranometer readings needs to be reconsidered. This study stressed the importance of considering these factors and developing appropriate correction algorithms to enhance the reliability of pyranometer measurements (Raïch *et al*. 2007). Martínez and colleagues in 2009 proposed a visible spectral range pyranometer that was affordable and effective. Their research resulted in a low-cost sensor capable of accurately measuring solar radiation (Martínez *et al*. 2009). Similarly, Medugu *et al*. in 2010 focused on constructing a reliable model pyranometer for irradiance measurements, contributing to the development of more precise solar radiation gauges (Medugu *et al*. 2010).

Furthermore, Xie *et al*. in 2010 conducted research on designing, fabricating, and characterizing CMOS MEMS-based thermoelectric power generators. They showcased the potential of these devices in converting waste heat into electrical energy, which could be beneficial for various applications, including solar pyranometers (Xie *et al*. 2010). Finally, In the year 2010, Wang and Zender conducted a study exploring the bias in MODIS snow albedo specifically under conditions of high solar zenith angles. Their study revealed a bias in MODIS snow albedo measurements during such angles, emphasizing the significance of accounting for solar zenith angles in accurate pyranometer measurements (Wange *et al*. 2010).

In 2011, Reda's exploration introduced a technique for approximating the ambiguity in quantifying shortwave solar irradiance employing thermopile and semiconductor solar radiometers (Reda *et al*. 2011). The subsequent year, Chow *et al*. directed their attention towards the near-future prognosis of photovoltaic energy production via an astute strategy (Chow *et al*. 2012). Likewise, Paul's examination in 2012 unveiled a rudimentary device for versatile measurements of various thermoelectric parameters (Paul B. 2012). In a similar manner, Sengupta scrutinized the efficacy of photodiode and thermopile pyranometers for photovoltaic applications in the same year (Sengupta, 2012). The 2012 research by Kim *et al*. plunged into the conceptualization of solar radiation utilizing silicon solar modules (Kim *et al*. 2012).

Numerous studies have examined the design and performance of photodiode-based pyranometers. For instance, Patil, Haria, and Pashte developed and assessed the performance of a photodiode-based pyranometer in measuring solar radiation accurately (Patil *et al*. 2013). Pandey and Katiyar focused on various solar radiation models and measurement techniques, providing insights into different approaches (Pandey and Katiyar, 2013). Muñoz-García *et al*. designed a low-cost sensor that precisely measured solar radiation within tree canopies, enabling a better understanding of shading's impact on solar energy systems (Muñoz-García *et al*. 2014). Geuder *et al*. delved into the enduring conduct, precision, and fluctuation of LI-200 pyranometers as radiation detectors within revolving shadow band irradiometers, furnishing valuable insights into the functionality and dependability of these devices (Geuder *et al*. 2014). HAFID and team devised a thermopile-centric pyranometer tailored for comprehensive spectrum solar irradiance assessment, with the intent to enhance precision and dependability across a multitude of wavelengths (HAFID *et al*. 2014).

Recently, there has been a growing interest in the development of affordable pyrometers using locally available materials (Osinowo *et al*. 2019). These pyrometers provide a cost-effective alternative to traditional solar radiation measurement devices, making them accessible to researchers and practitioners in developing nations. In 2014, a remarkable investigation was undertaken by Daniel Asiegbu and Echeweozo Odinakachi, whose study cantered on the creation, fabrication, and alignment of a solar irradiance gauge. The study demonstrated the accuracy of their design in measuring solar radiation levels, making it a valuable tool for solar energy systems and related applications (Daniel *et al*. 2014). Frank Vignola also examined the evaluation of the diffuse response of pyranometers based on solar cells. The study analyzed the performance of these pyranometers in measuring diffuse solar radiation, a crucial parameter for solar energy applications (Vignola). Furthermore, Norbert Geuder, Roman Affolter, Maria Eckl, Birk Kraas, and Stefan Wilbert investigated the accuracy and precision of twin-sensor rotating shadow band irradiometers (RSIs) in measuring solar irradiance (Geuder *et al*. 2012). They also evaluated these instruments' overall performance in solar irradiance measurement. Muhammad Shafa and colleagues conducted research on a low-cost pyranometer with a wide range of measurement capabilities in 2015 (Shafa *et al*. 2015). They also validated the pyranometer's credibility by comparing its measurements with those obtained from a standard pyranometer.

Precise calibration of rotating shadow band irradiometers (RSIs) is crucial for accurately measuring solar irradiance. Jessen *et al*. (2015) carried out a study evaluating different calibration methods for RSIs and the impact of calibration duration. Their discoveries pointed out that extended calibration durations yielded heightened precision in measurements, especially concerning scattered irradiance (Jessen *et al*. 2015). Likewise,

Srikrishnan and colleagues proposed the utilization of multi-pyranometer arrays alongside neural networks for the estimation of direct normal irradiance (DNI). They formulated a framework leveraging data from numerous pyranometers to forecast DNI with exceptional accuracy, thereby augmenting DNI estimation for the design and functioning of solar energy systems (Srikrishnan *et al*. 2015)

In a different approach, Dumitrescu *et al*. introduced a solid-state pyranometer as an alternative to traditional pyranometers. The compact size, low cost, and high durability of the solid-state pyranometer make it a promising choice. The authors conducted experiments to validate its performance and confirmed its accuracy in measuring solar radiation (Anca *et al*. 2015). In a Nigerian study, Nwankwo and Nnabuchi developed a locally made pyranometer for measuring global solar radiation. The results demonstrated that the pyranometer offered reliable measurements, making it a cost-effective solution for solar energy applications in Nigeria (Nwankwo *et al*. 2015).

Agawa and Ibrahim (Agawa *et al*. 2016) engineered a surveillance mechanism for an autonomous photovoltaic setup, employing a microcontroller. As per research conducted by Orsetti and team, a cost-effective and dependable solar irradiance gauging system is put forth. This setup integrates economical pyranometers for the assessment of wide-ranging solar radiation (Orsetti *et al*. 2016). Similarly, Michalsky *et al*. address the issue of nighttime offsets in pyranometers. They present a solution in the form of a high-flow DC ventilation system to reduce these offsets, thereby improving measurement accuracy during nighttime conditions (Michalsky *et al*. 2017). In the research by Vignola, the focus shifts towards the elimination of biases in rotating shadow band radiometers (RSRs). The author proposes methods to mitigate these biases (Vignola *et al*. 2019). Tohsing *et al*. emphasize the importance of cost-effective measurement devices for the widespread implementation of solar irradiance measurement systems. They introduce the creation of a low-cost pyranometer designed to measure broadband solar radiation (Tohsing *et al*. 2019).

Walter-Shea *et al*. propose improvements in the calibration process of silicon photodiode pyranometers, aiming to enhance solar irradiance measurement systems (Walter-Shea *et al*. 2019). Additionally, Moiz *et al*. (2020) focus on enhancing the performance of a PEDOT: PSS-silicon nanowire-based hybrid solar cell by integrating silicon nanowires into the device structure. They achieve this by creating a silicon nanowire array using a metal-assisted chemical etching method and coating the nanowires with a layer of PEDOT: PSS as a hole transport material (Moiz *et al*. 2020).

From the literature review it is concluded that thermopiles cannot be completely substituted due to various challenges encountered, such as the occurrence of dark current in the absence of light, operations depending on temperature, and saturation at elevated irradiance levels. In the proposed methodology, a novel design of a photodiode based pyranometer has been devised to overcome these challenges by incorporating a data acquisition system and correction technique. This innovative method offers a practical solution for independent solar radiation measurement, enhancing precision and dependability. The investigation presented herein contrasts the performance of a photodiode pyranometer with that of a conventional pyranometer under overcast conditions. The behaviour of the photodiode pyranometer mirrors the abrupt drops observed in the standard pyranometer, exhibiting brief spikes influenced by the magnitude of the correction function. While the uncorrected pyranometer tends to overestimate irradiance, a first-order linear correction effectively addresses this issue. Notably, corrections ranging up to the seventh order led to a discrepancy of ±10 W/m^2, indicating that corrections of the third to fifth degree may offer optimal outcomes. A quaternary function could potentially serve as the most effective correction method, although higher order polynomials also demonstrate efficacy.

2. Design of photodiode pyranometer

The significance of the pyranometer's casing design cannot be underestimated. The mechanical structure is made of mild steel and its design is simple. The casing has a circular base with a thickness of 6 mm and a diameter of 110 mm. On the surface of the circular disc, there is a cylinder with a diameter of 63 mm and a threaded end. To ensure proper leveling, three holes of each Ø$^{3/8}$ were drilled and nuts were welded onto them. Adjustments to the casing's leveling are made by manipulating the levelling screws according to the position of the spirit level. Additionally, a central hole with a diameter of Ø$^{3/8}$ was drilled to accommodate the terminal contact, which establishes a connection to the photodiode. To maintain a constant temperature within the instrument, the outer casing of the pyranometer is designed to be heavy. To prevent corrosion, the casing's surface is coated with a layer of powder coating. The choice of white colour specifically for the coating is based on its ability to reflect most of the light's spectral wavelengths. The photodiode assembly is surrounded by thermal insulation to prevent excessive heating of internal components.

Please refer to Figure 1(a-c) for images depicting the initial and final finished casing. Additionally, Figure 1 provides an illustration of the internal structure of the designed pyranometer.

3. Calibration of designed pyranometer

3.1. Calibration of silicon photodiode pyranometer

Figure 2 illustrates the placement of the photodiode pyranometer on the calibration table, alongside the Eppley PSP pyranometer, which is a second-class high-precision thermopile-based instrument. The calibration of the photodiode pyranometer is carried out using the radiation transfer model of the World Meteorological Organisation (WMO). To conduct the calibration, both the test pyranometer and the standard Eppley pyranometer are connected to the Geonica 3000C high-resolution data

logger, which provides a resolution of up to 24 bits at 2.5V. Data is collected every second and averaged over a 1-minute period. In addition to measuring the irradiation in millivolts, the automated 2-axis solar tracker fitted with a Pyrheliometer from Geonica Earth Sciences also records the solar elevation. The calibration process takes place during March-April 2023, ensuring a balanced combination of clear and cloudy sky conditions.

4. Results and discussion

In result and discussion, the elaboration has been made through the polynomial correction function calculations, correlation analysis and error calculation.

4.1. polynomial correction function calculation and regression analysis

The polynomial function fitting was applied to the data using the least square method up to the seventh order. To analyze the daily measurements, regression analysis was performed for the entire dataset. Figure 3 illustrates the regression fit for the daily data of March 13, 2023. The scatter plot of the data indicates a linear relationship between the measured irradiance using the thermopile and photodiode. The averaged coefficients for the empirical linear polynomial fit at different degrees are provided in Table 1 and Table 2. By substituting the response of the photodiode pyranometer in the correction function, we obtained the corresponding corrected values for the response. If the polynomial correction is employed, then the irradiance from the photodiode pyranometer is expressed as:

$$E_{PD} = a_o + \sum_{i=1}^{n} a_i (R_{PD})^i \quad (1)$$

$$E_{PD} = a_0 + a_1 R_{PD} + a_2 R_{PD}^2 + \ldots + a_{n-1} R_{PD}^{n-1} + a_n R_{PD}^n \quad (2)$$

Where EPD is the irradiance measured with photodiode pyranometer, ao – an is the coefficients of the polynomial terms till the order of n, RPD is the response voltage produced by the photodiode for the corresponding irradiance.

Table 1. Averaged coefficients of polynomial correction (till order 3)

Coefficients of polynomial function	Degree of polynomial			
	Uncorrected × 10^3	1st order × 10^3	2nd order × 10^3	3rd order × 10^3
a_0	0	0.05920	0.0101	0.0108
a_1	13.2067	12.1353	16.9715	18.5773
a_2			-44.1232	-131.9489
a_3				743.5038

Table 2. Averaged coefficients of polynomial correction (till order 7)

Coefficients of polynomial function	Degree of polynomial			
	4th order × 10^3	5th order × 10^3	6th order × 10^3	7th order × 10^3
a_0	0.0039	0.0014	-0.0320	-0.0299
a_1	15.9953	16.8695	25.8771	24.7934
a_2	-9.5449	-46.2146	-879.7884	-711.5376
a_3	-137.0807	-959.6733	32792.9333	21304.8000
a_4	12014.8139	14502.1267	-651432.6666	-258033.3333
a_5		-45309.1000	-0.0022E7	-811896.6666
a_6			-0.00164E7	0.0041E7
a_7				-0.0022E10

4.2. Correlation analysis of the polynomial correction functions

The selection of the ideal polynomial function for correction can be done through correlation analysis. By plotting the irradiance from the standard and photodiode pyranometer in a scatter plot with a reference line of 45°, as discussed earlier, we can examine the correlation. In Figure 4, we can observe the correlation plot of the irradiance measurements taken on March 11, 2023. The presence of data points above the 45° line indicates a perfect correlation with the standard measurement. In the case of the uncorrected photodiode pyranometer, the data points align perfectly with the line at lower irradiance levels, but at higher irradiance, there is more deviation, suggesting the need for correction When implementing a first-order correction, an offset is introduced causing a deviation from the 45° line at lower irradiance levels. However, at irradiance levels ranging from 600-1000 W/m^2, the data points overlap. Similarly, the quadratic correction yields a perfect overlap in the range of 0-450 W/m^2, but deviations occur at higher irradiance levels (>450 W/m^2). The cubic correction shows a perfect correlation in the ranges of 0-450 W/m^2 and 800-1000W/m^2, but there is a wide deviation in the range of 450-800 W/m^2, indicating that the function lacks effectiveness in medium irradiance conditions. On the other hand, the quaternary correction function provides better correlation at medium irradiance levels compared to the cubic model, while exhibiting similar responses at lower and higher irradiance levels. Furthermore, the fifth-degree polynomial correction demonstrates slightly improved correlation at both lower and higher irradiance levels. However, increasing the degree of the polynomial correction beyond the fifth degree shows no further improvement.

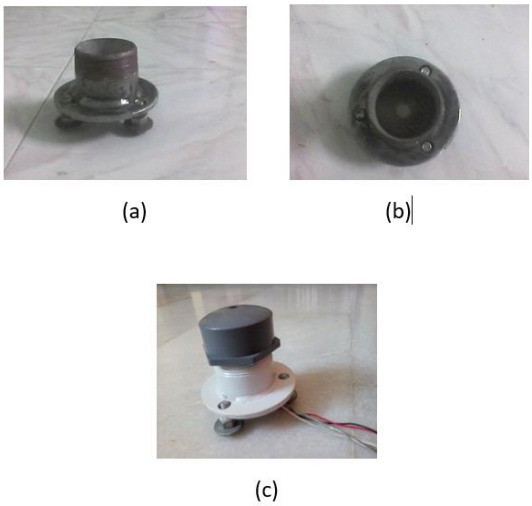

(a) (b)

(c)

Figure 1. Unfinished (a-b) and finished (c) outer casing of pyranometer

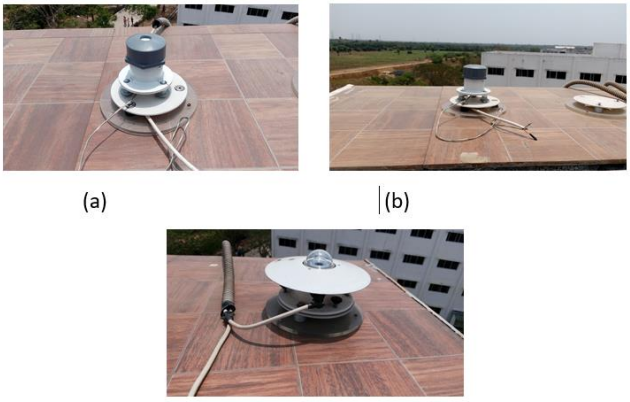

(a) (b)

(c)

Figure 2. Photodiode pyranometer and Eppley PSP pyranometer mounted on the calibration

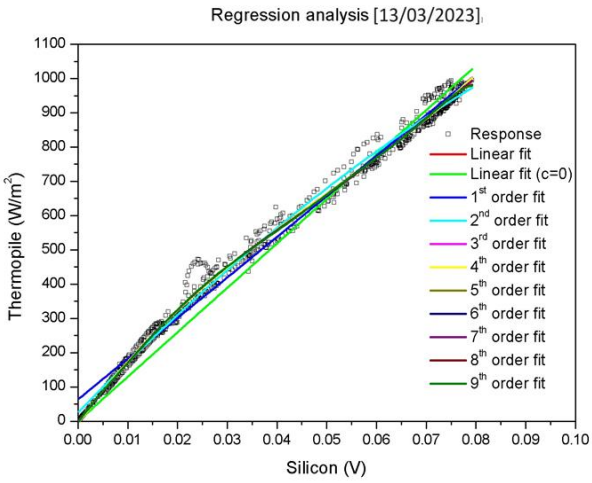

Figure 3. Regression fit for irradiance on March 13, 2023

To gain a clearer understanding, the correlation coefficient was examined with increasing degrees of polynomial correction. Figure 5 illustrates the variation of the regression coefficient with the degree of correction function. The line representing the correlation coefficient (R^2 = 0.9914) corresponds to the uncorrected photodiode pyranometer. This coefficient indicates the proximity of the data points to the equation of the fitted line. As seen in Figure 4, the correlation coefficient increases from linear (R^2 = 0.98869) to quadratic (R^2 = 0.98973), and there is a sharp increase for the cubic (R^2 = 0.99721) polynomial correction. Additionally, the correlation coefficient remains almost the same for degrees three to five. Further increasing the degree of the correction function leads to a coefficient of 0.99969. However, the seventh-degree correction exhibits an abnormal drop to 0.99594.

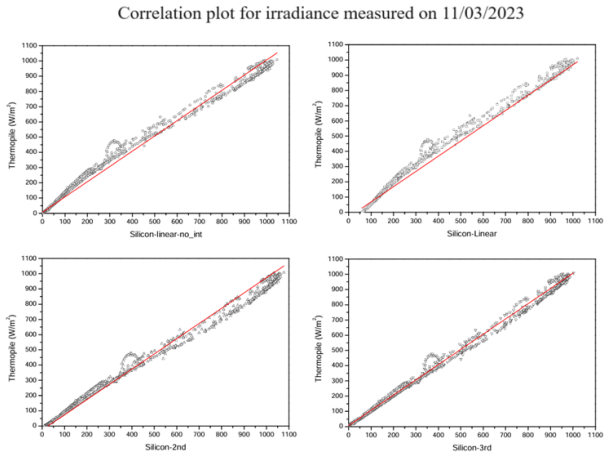

Figure 4. Correlation plot for irradiance measured on March 11, 2023 (till 3rd order)

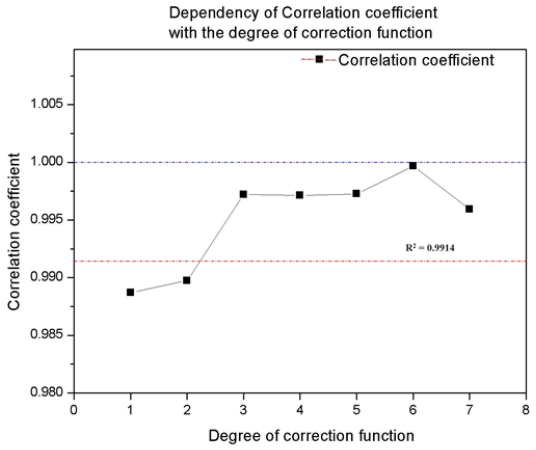

Figure 5. Variation of correlation coefficient with degree of correction

This abnormal variation in the correlation coefficient can be attributed to greater uncertainty associated with larger coefficients, resulting in significant errors when using high-degree polynomial functions for correction. Moreover, the coefficients are calculated with a standard error, indicated as a horizontal error bar on the data points. When these coefficients are calculated with larger errors, it leads to distortions in the derived corrections. Therefore, corrections of degrees three to five are deemed suitable for achieving effective correction of the photodiode pyranometer.

4.3. Error analysis

The computation of percentage error/difference was done specifically for solar zenith angles greater than 80° due to the distortions caused by higher zenith angles on the corrections. Any abnormal values in the differences were eliminated from the calculation dataset. Figure 6 illustrates the percentage difference for all the

uncorrected/corrected data sets. Uncorrected irradiance results in an error of 7.97%. The error is significantly reduced to 2.28% through linear correction. However, the quadratic correction abnormally leads to an error of approximately 8.64%. This unusual error occurs because the quadratic function fails to properly correct medium and higher irradiance values. On the other hand, using a fourth-degree polynomial function yields a lower error of 0.91%. Increasing the degree of the polynomial further raises the error from 0.91% to 3.13%. Thus, a quaternary function appears to be the optimal correction function, although higher order polynomials can also perform equally well. Generally, avoiding higher order corrections is preferred due to the larger coefficients and standard error involved in their calculations.

The difference in percentage between standard and photodiode pyranometer is obtained by

$$\%Difference = \left(\frac{E_{PD} - E_{TH}}{E_{TH}} \right) \times 100\% \quad (3)$$

Where EPD is the irradiance measured with photodiode pyranometer and ETH is the irradiance measured with thermopile based Eppley PSP pyranometer. The abnormal data sets are excluded during the error calculation.

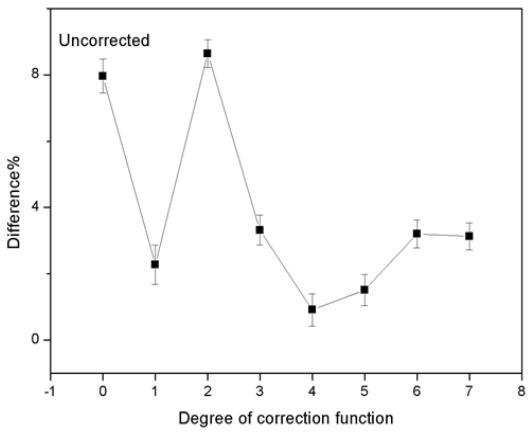

Figure 6. Variation of % difference with degree of correction polynomial

5. Conclusion

The improved silicon photodiode pyranometer shows a maximum accuracy of 91% for instantaneous measurements. These findings offer a viable alternative to conventional thermopile-based pyranometers, allowing silicon pyranometers to effectively measure irradiance. Moreover, photodiode pyranometers are advantageous due to their compact size, lightweight design, and low production costs. Additionally, their rapid response time enables faster and more precise instantaneous measurements. The study compares the response of a photodiode pyranometer to a standard pyranometer under dynamic irradiance conditions. The photodiode pyranometer mimics the sharp declines observed in the standard pyranometer, with transient increases dependent on the correction function's magnitude. The uncorrected pyranometer displays a 50 W/m^2 variation in irradiance levels between 14:30 -15:00 hours, which diminishes to 2 W/m^2 post the integration of all correction functions. The quadratic function continues to overestimate irradiance, suggesting its unsuitability for the photodiode pyranometer. Corrections up to the seventh order result in a ±10 W/m^2 difference around the null point, indicating that third to fifth-degree correction functions could be optimal. The correlation coefficient line (R^2 = 0.9914) corresponds to the uncorrected photodiode pyranometer, with a progressively increasing correlation coefficient from linear to quadratic and cubic to seventh-order correction.

6. Future work

The field of material sciences continues to introduce ground breaking discoveries that bring forth new materials with unique characteristics and qualities. These innovations enable the engineering of the band gap in semiconductors to effectively function across the entire spectrum of solar radiation. Consequently, this alteration in the band gap of semiconductors empowers the resulting devices to capture a wide range of solar spectrum. In the pursuit of improved performance, the inclusion of correction factors based on solar zenith angles, angle of incidence, and temperature can greatly enhance the capabilities of photodiodes.

Absolutely, advancements in material science have indeed led to remarkable discoveries in manipulating semiconductor properties, particularly in adjusting band gaps for efficient operation across various solar radiation wavelengths. By modifying the band gap, semiconductor devices can effectively harness a broader spectrum of solar energy, enhancing their performance in photovoltaic applications.

Moreover, integrating correction parameters such as solar zenith angles, angle of incidence, and temperature into the design and operation of photodiodes can further optimize their functionalities. These parameters play crucial roles in determining the amount and quality of solar radiation reaching the photodiode, and by accounting for them, engineers can improve the accuracy and efficiency of photodiode-based systems, such as solar panels or sensors. Overall, these advancements not only expand our understanding of semiconductor physics but also offer practical solutions for improving renewable energy technologies.

References

Aakanksha P., Kartik H. and Priyanka P. (2013). Photodiode Based Pyranometer, *International Journal of Advances in Science Engineering and Technology*, ISSN: 2321–9009, 1, (1), July–2013.

Agawa Y. and Ibrahim S.B. (2016). Development of Microcontroller Based Monitoring System for a Stand-Alone Photovoltaic System, *Nigerian Journal of Technology* (NIJOTECH), **35**, No. 4, 904–911, http://dx.doi.org/10.4314/njt.v35i4.27.

Beaubien D.J.A., Bisberg and Beaubien A.F. (1998). Investigations in Pyranometer Design. *Journal of Atmospheric and Oceanic Technology*. https:// doi.org/10.1175/ 1520-0426.

Biplab P. (2012). Simple Apparatus for the Multipurpose Measurements of Different Thermoelectric Parameters. *Measurement* **45** (1): 133–39.

Bush Brett C., Francisco P.J. Valero A., Simpson S. and Lionel Bignone. (2000). Characterization of Thermal Effects in Pyranometers: A Data Correction Algorithm for Improved Measurement of Surface Insolation. *Journal of Atmospheric and Oceanic Technology*. https://doi.org/10.1175/1520-0426.

Chow Stanley K.H., Eric W.M Lee. and Danny H.W.Li. (2012). Short-Term Prediction of Photovoltaic Energy Generation by Intelligent Approach. *Energy and Buildings* **55** (December): 660–67.

Daniel., Asiegbu A. and Echeweozo E. Odinakachi. (2014). Design, Construction and Calibration of a Solar Radiation Measuring Meter. *Review of Advances in Physics Theories and Applications* **1** (1): 1–8.

Dumitrescu A.L., Paulescu M. and Ercuta A. (2015). A Solid State Pyranometer, Analele Universităţii de Vest din TimişoaraVol. LVIII, Seria Fizică. DOI: 10.1515/awutp -2015-0207.

Frank Vignola, Solar Cell Based Pyranometers: Evaluation of The Diffuse Response.

Geuder N., Affolter R., Eckl M., Kraas B, Wilbert S. (2012). Measurement Accuracy of Twin-SensorRotating Shadowband Irradiometers (RSI), SolarPACES Conference, Marrakesh, Morocco.

Geuder N., Affolter R., Kraas B. and Wilbert S. (2014). Long-Term Behavior, Accuracy and Drift of LI-200 Pyranometers as Radiation Sensors in Rotating Shadowband Irradiometers (RSI). *Energy Procedia* **49**: 2330–39.

Haeffelin M., Kato S., Smith A.M., Rutledge C.K., Charlock T.P. and Mahan J.R. (2001). Determination of the Thermal Offset of the Eppley Precision Spectral Pyranometer. *Applied Optics* **40** (4): 472–84.

HAFID A.A., MEDDAH K., ATTARI M. and REMRAM Y. (2014). A Thermopile Based Pyranometer for Large Spectrum Sunlight Measurement, International Conference on Embedded Systems in Telecommunications and Instrumentation (ICESTI'14), Annaba, Algeria, October, 27–29, 2014.

Jessen W., Wilbert S., Nouri B., Geuder N. and Fritz H. (2015). Calibration Methods for Rotating Shadowband Irradiometers and Evaluation of Calibration Duration. https://doi.org/10.5194/amtd-8-10249-2015.

Kim J.Y., Seung-Hwan Y., Lee C., Young-Joo K, Hak-Jin K., Seong In Cho, Joong-Yong R. (2012). Modeling of Solar Radiation Using Silicon Solar Module, *Journal of Biosystems Engineering*, http://dx.doi.org/10.5307/JBE.2012.37.1.011.

Link., Timothy E., Marks D. and Janet P. Hardy. (2004). A Deterministic Method to Characterize Canopy Radiative Transfer Properties. *Hydrological Processes* 18 (18): 3583–94.

Martínez., Miguel A., José M. Andújar and Juan M. Enrique. (2009). A New and Inexpensive Pyranometer for the Visible Spectral Range. Sensors 9 (6): 4615–34.

Medugu Medugu W.D., Burari W.F., Abdulazeez. and A.A. (2010). Construction of a Reliable Model Pyranometer for Irradiance Measurements. *African Journal of Biotechnology*. https://doi.org/10.5897/ajb10.030.

Michalsky, Joseph J., Kutchenreiter M. and Long C.N. (2017). Significant Improvements in Pyranometer Nighttime Offsets Using High-Flow DC Ventilation. *Journal of Atmospheric and Oceanic Technology* 34 (6), 1323–32.

Muhammad S., Luo S., Tong X., Farooq M.U., Gao L. and Zhou Z. (2015). Low Cost Pyranometer for Broad Range and Its Credibility Check with Standard Pyranometer. J*ournal of Nanoelectronics and Optoelectronics* 10 (1): 119–25.

Muñoz-García M.A., Melado-Herreros A., Balenzategui J.L. and Barrerio P. (2014). Low-Cost Irradiance Sensors for Irradiation Assessments inside Tree Canopies. Solar Energy 103 (May): 143–53.

Nwankwo S. and Nnabuchi M.N. (2015). Global Solar Radiation Measurement in Abakaliki Ebonyi State Nigeria Using Locally Made Pyranometer, International Journal of Energy and Environmental Research 3, 2, 47–54, September 2015.

Orsetti C., Muttillo M., Parente F.R., Pantoli L., Stornelli V. and Ferri G. (2016). Reliable and Inexpensive Solar Irradiance Measurement System Design. Procedia Engineering 168: 1767–70.

Osinowo M.O., Willoughby A.A., Ewetumo T., Kolawole L.B, (2019). Development of a Low-Cost Pyrometer using Locally Sourced Materials, International Journal for Scientific Research & Development|, 7, (05).

Pandey C.K. and Katiyar A.K. (2013). Solar Radiation: Models and Measurement Techniques, Journal of Energy, http://dx.doi.org/10.1155/2013/305207.

Raïch. (2007). Effects of Solar Height, Cloudiness and Temperature on Silicon Pyranometer Measurements. Tethys Journal of Weather and Climate of the Western Mediterranean 4. https://doi.org/10.3369/tethys.2007.4.02.

Reda I. (2011). Method to Calculate Uncertainty Estimate of Measuring Shortwave Solar Irradiance Using Thermopile and Semiconductor Solar Radiometers. https://doi.org/10.2172/1021250.

Sengupta M. (2012). Evaluation of Photodiode and Thermopile Pyranometers for Photovoltaic Applications:

Srikrishnan V., George S. Young, Lucas T. Witmer. and Jeffrey R.S. and Brownson. (2015). Using Multi-Pyranometer Arrays and Neural Networks to Estimate Direct Normal Irradiance. Solar Energy 119 (September): 531–42.

Syed Abdul A.N.M. Alahmadi and Abdulah Jeza Aljohani A.J. (2020). Design of Silicon Nanowire Array for PEDOT: PSS-Silicon Nanowire-Based Hybrid Solar Cell. Energies. https://doi.org/10.3390/en13153797.

Tohsing K., Phaisathit D., Pattarapanitchai S., Masiri I., Buntoung S., Aumporn O. and Wattan R. (2019). A development of a low-cost pyranometer for measuring broadband solar radiation, Journal of Physics: Conference Series 1380. 012045, doi:10.1088/1742-6596/1380/1/012045.

Vignola F. (2019). Removing Biases from Rotating Shadowband Radiometers: Preprint.

Walter-Shea, Elizabeth A., Hubbard K.G., Mesarch M.A. and Roebke G. (2019). Improving the Calibration of Silicon Photodiode Pyranometers. Meteorology and Atmospheric Physics. https://doi.org/10.1007/s00703-018-0624-3.

Wang X. and Zender C.S. (2010). MODIS Snow Albedo Bias at High Solar Zenith Angles Relative to Theory and to in Situ Observations in Greenland. Remote Sensing of the Environment 114 (3): 563–75.

Wood J., Tariq M. and Kubie J. (2003). Evaluation of a New Photodiode Sensor for Measuring Global and Diffuse Irradiance, and Sunshine Duration. Journal of Solar Energy Engineering. https://doi.org/10.1115/1.1531149.

Xie J., Chengkuo L. and Hanhua F. (2010). Design, Fabrication, and Characterization of CMOS MEMS-Based Thermoelectric Power Generators. Journal of Micro electromechanical Systems: A Joint IEEE and ASME Publication on Microstructures, Micro actuators, Micro sensors, and Microsystems 19 (2): 317–24.